



Ultrafast laser writing quill effect in low loss waveguide fabrication regime

JUN GUAN,^{1,3} XIANG LIU,¹ AND MARTIN J. BOOTH^{1,2,*}

¹ Department of Engineering Science, University of Oxford, Parks Road, Oxford OX1 3PJ, UK

² Centre for Neural Circuits and Behaviour, University of Oxford, Mansfield Road, Oxford OX1 3SR, UK

³ jun.guan@eng.ox.ac.uk

*martin.booth@eng.ox.ac.uk

Abstract: The quill effect is a laser writing phenomenon in which different fabrication effects occur, depending upon the direction of laser translation. It has not yet, to our knowledge, been studied in the low-loss-waveguide (LLW) writing regime, probably due to its very weak visibility under conventional transmission microscope in that regime. In this report, with the help of adaptive third harmonic generation microscopy, we reveal the quill effect in the LLW writing regime and show its influences on the properties of laser-written photonic integrated components, in terms of polarization-related properties in fused silica and beam-splitting ratios of three-waveguide-coupler in borosilicate glass.

Published by The Optical Society under the terms of the [Creative Commons Attribution 4.0 License](#). Further distribution of this work must maintain attribution to the author(s) and the published article's title, journal citation, and DOI.

1. Introduction

The quill effect [1], which manifests as a change in material modification when reversing the writing direction of ultrafast laser direct writing, has been actively studied over the last decade since it was reported by Poumellec and associates [2]. Kazansky et al. suggested the quill effect arises from pulse front tilt (PFT) of the writing beam [1], which is supported by following works [3–5]. This was expanded upon by Salter et al., by showing that both PFT and time-invariant focal asymmetry may give rise to the quill effect [6]. So far all prior works predominately focused on quill effects arising in laser irradiated regions in fused silica that exhibited damage-like structures and were fabricated well above the low-loss-waveguide (LLW) writing regime [1–9]. In the damage-causing fabrication regime, the quill effect was clearly visible under a transmission mode microscope, but this fabrication regime is not particularly useful for functional photonic components. Understanding the quill effect in the LLW writing regime and in both fused silica and another commonly used glass-borosilicate glass [10–14] is very important for the design and fabrication of femtosecond-laser-written photonic integrated circuits (FLW-PIC). Such highly demanding applications in this area include polarization sensitive quantum information processing based upon photons [11–15], which impose strict requirements on the polarization properties of the fabricated FLW-PIC components. We find that the quill effect have noticeable influence on such properties.

In this report, by means of adaptive third harmonic generation (THG) microscopy [16,17], we visualize the quill effect in LLW writing regime and reveal its influence on the polarization-related properties of low loss waveguides in fused silica, as well as on the beam-splitting-ratios of a three-waveguide-coupler (tritter) in borosilicate glass.

2. Experiment

The laser that was employed to write FLW-PIC components inside glass was the second harmonic of a regenerative amplified Yb:KGW laser (Light Conversion Pharos SP-06-1000-pp) with 1 MHz repetition rate, 514 nm wavelength and 170 fs pulse duration. The power of

the laser beam was regulated through the combination of a motorized rotating half waveplate and a polarization beam splitter before being circularly-polarized and focused 120 μm below the top surface of the glass chip with a 0.5 NA objective lens. The glass chip, which was fixed on a three-axis air bearing stage (Aerotech ABL10100L/ABL10100L/ANT95-3-V), was transversely scanned relative to the focus to inscribe FLW-PIC components. The custom-built adaptive THG microscope was as described in [16]. Aberrations were corrected through sequential adjustment of the amplitudes of the Zernike polynomial modes added to the deformable mirror, in order to maximize an image quality metric, which was defined as the total image intensity. Both the system aberrations resulting from the microscope light path and the sample-introduced aberrations were corrected. The lateral resolution of this THG microscope is better than 500 nm; its axial resolution is around 1.3 μm [17]. We note here that while the THG depends upon the third-order non-linear optical properties of the material, in practice the measured THG signal correlates spatially to changes in refractive-index profiles [17,18], such that a rapid spatial transition between different refractive indices typically correlates with a high signal. During light-coupling tests, a 780 nm-wavelength laser beam from a polarization-maintaining fiber-coupled laser source (Thorlabs S1FC780PM) was butt-coupled into waveguide through a polarization-maintaining fiber (Thorlabs P1-630PM-FC-5); a photodiode power sensor was used to measure the power. The polarization states of the input and output beams into and from a waveguide were measured with a polarimeter (Polarization Analyzer SK010PA-VIS, Schäfter + Kirchhoff GmbH). Propagation losses were measured through the cutback approach.

2.1 Quill effect in LLW writing regime in fused silica

In fused silica (LEONI SQ0), three pairs of waveguides were written with the same scan speed of 10 $\mu\text{m/s}$ and sample-surface-level pulse energy of 23.6, 25.2 and 26.8 nJ respectively; within each pair, two waveguides were written the same writing parameters except in opposite scan directions. All the waveguides were written in the same chip to reduce the influences of writing system drift and material non-uniformity, as well as to guarantee the same waveguide length for all waveguides. Their cross-sectional THG images are shown in Fig. 1(a), where we can see that for the pair written with pulse energy of 23.6 nJ, both the THG profiles and signal strengths of their THG images were clearly different, which contrasted with the similarity between their transmission microscope images in Fig. 1(a); at a pulse energy of 25.2 nJ, their THG signal strengths were still different but their THG profiles became closer in form; as the pulse energy was increased to 26.8 nJ, both their THG signal strengths and profiles became more similar.

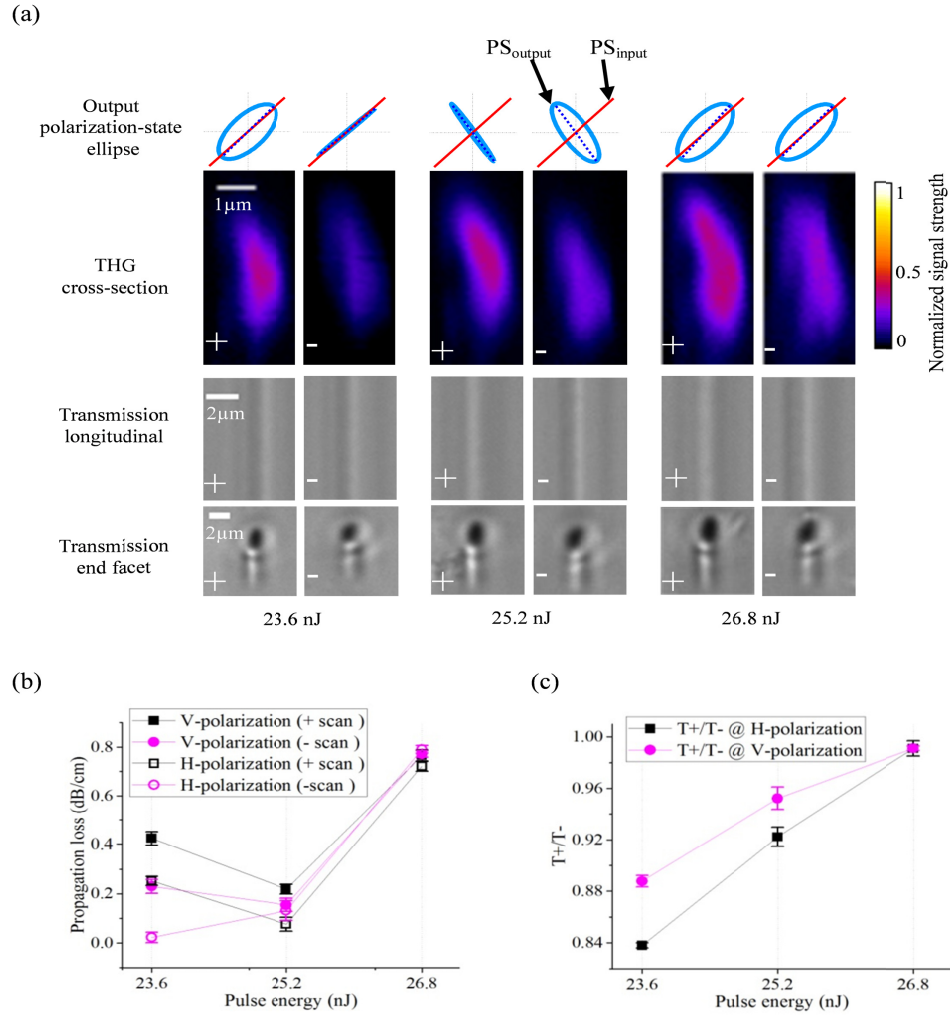


Fig. 1. Quill effect in LLW writing regime in fused silica. (a) Measured output polarization state (PS_{output} , represented by polarization state ellipse) with respect to that of input (PS_{input}) (top row); cross-sectional THG images of the three pairs of waveguide (the second row, in false color), which were taken with the same THG microscope settings; '+' and '-' denote opposite scan directions; corresponding longitudinal (the third row) and end-facet (bottom row) transmission microscope image. Chip length is 13.3 mm. (b) Measured propagation loss at horizontal (H-polarization) and vertical (V-polarization) polarization; the error bars represent peak-to-valley variation of multiple tests. Before and after cutback the polished chip lengths are 38.3 mm and 13.3 mm respectively. (c) Ratio between measured throughputs of a pair of waveguides at horizontal and vertical polarization; T_+ and T_- represent throughputs of waveguide written in '+' and '-' scan directions respectively.

This qualitative THG trend correlated with following four measured quantitative trends: I: polarization modulation, which is represented by the measured polarization-state ellipse of the output light (PS_{output}) with respect to that of the input light (PS_{input}), as shown in the top row figures of Fig. 1(a); PS_{input} was kept unchanged during measurements of all waveguides; II: propagation losses in horizontal and vertical polarization directions as shown in Fig. 1(b); III: the throughput ratio T_+/T_- at horizontal and vertical polarization directions in Fig. 1(c) T_+ and T_- denote throughputs of waveguides written in opposite directions within a pair; IV: the waveguide output near field mode profile at horizontal and vertical polarization of input light as shown in Fig. 2; in Fig. 2(b), D_x/D_y is the ratio between the diameters of a mode profile

along x-axis (D_x) and y-axis (D_y); the difference between D_x/D_y at horizontal polarization and that at vertical polarization decreased as pulse energy was increased from 23.6 to 26.8 nJ. We note that in Fig. 1(b) the measured propagation loss of the waveguide written with pulse energy of 23.6 nJ and ‘-’ scan direction was well below 0.1 dB/cm when it was tested with horizontal polarization 780 nm laser. Although we had verified it with repeated experiments and multiple tests, we are cautious to specify its value considering that the measurement accuracy of cutback approach depends on the waveguide length and coupling repeatability especially at low propagation loss and the longest chips we used were only 40 mm long.

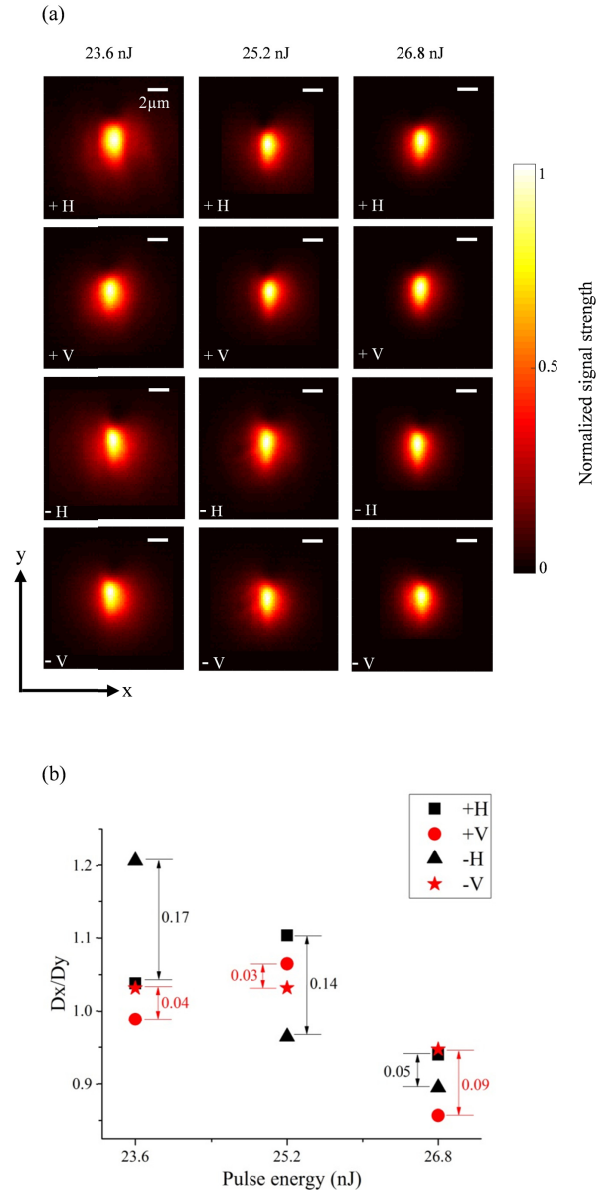


Fig. 2. Output near field mode profiles of waveguides at horizontal and vertical polarized input light. (a) Recorded near field mode profile images; images were intensity-normalized and in false color; all scale-bars represent 2 μ m. (b) D_x/D_y of waveguides; D_x and D_y are diameters of near field of mode profiles in x- and y- axis, where the diameter at the $1/e^2$ intensity points is

used; marked numbers are the D_x/D_y difference between waveguide written in opposite directions and tested in orthogonal polarizations.

As one can see from Fig. 1 and Fig. 2, the optical properties of waveguides, whose variations correlate to that of THG images under quill effect, are polarization related. To understand these correlations and quill effect in the LLW regime, we start from the origins of polarization-dependency of those waveguides. There are three known types of birefringence in femtosecond laser written waveguides in fused silica [19]: shape birefringence [20], stress-induced birefringence [21] and birefringence induced by nanograting structures [22]. It has been proven that circular polarization [23] of writing beam or repetition rates over 500 kHz [24], which both are the case in this report, can be used to avoid the birefringence induced by nanograting structures. Therefore, it is reasonable that we only consider shape and stress-induced birefringence in the waveguides shown in Fig. 1. Obviously shape birefringence results from the noncircular cross-sectional shape of a waveguide; but stress-introduced birefringence also originates from the noncircular or non-uniform cross-sectional profile of waveguide considering the isotropic properties of glass before being irradiated with femtosecond laser. Both shape and stress-introduced birefringence in laser writing single mode waveguides are similar to that of the single mode fiber, in term of birefringence formation mechanisms. Therefore, based on the study on birefringence of single mode fiber [25,26], both shape birefringence and stress-introduced birefringence of waveguides depend on their profiles that are correlated to their THG image [17]. Based on the relationship between propagation loss, coupling loss and throughput at orthogonal polarizations of input light, as well the relationship between refractive index change and near field mode diameters at orthogonal polarizations [19], the correlations between THG images shown in Fig. 1(a) and the optical properties shown in Figs. 1(b) and 1(c) and Fig. 2 can be understood.

2.2 Quill effect in LLW writing regime in borosilicate glass

In borosilicate glass, another broadly used FLW-PIC substrate especially for applications like quantum information processing [11–14,27–29], to our knowledge, there has not yet been a detailed report of the quill effect, in particular at MHz repetition rates of writing laser, in spite of being mentioned in prior work [30]. As its softening temperature is lower than that of fused silica, consequently the thermal smoothing effect [31] can easily make the quill effect ‘invisible’ under a conventional transmission microscope. However, with the adaptive THG microscope we can reveal the ‘invisible’ quill effect. For demonstration, waveguides were written in Corning EAGLE 2000 glass at a pulse energy of 110 nJ and a scan speed of 0.3 mm/s. The cross-sectional profile of a waveguide is shown by its THG images in Fig. 3(a) alongside its transmission microscope image, in which the THG signal in the region at the bottom is much stronger than that in the upper parts of the waveguide. The bottom region with strong THG signal is believed to be due to a micro-explosion [32]. To show the quill effect more clearly, six waveguides were written with alternate scan directions, pulse energy of 110 nJ, scan speed of 0.3 mm/s and separation of 4 μm next to each other in x-axis; as shown in the transmission microscope image of the end-facet in Fig. 3(b), the close-up THG image of their bottom region is shown in Fig. 3(c), from which one can see the clear quill effect manifested through the THG signal strength contrast of waveguides written in opposite directions.

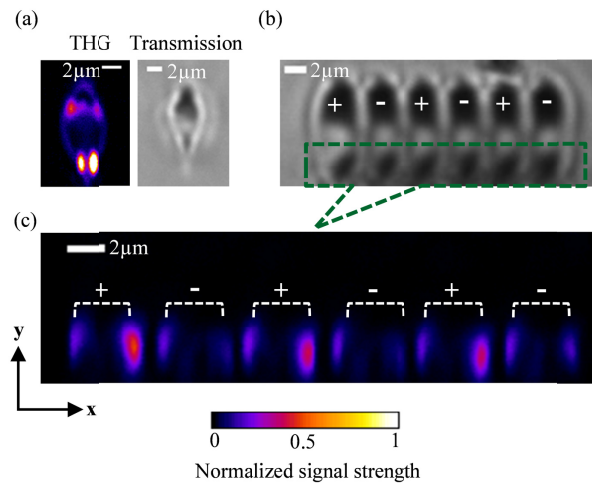


Fig. 3. Quill effect in Corning EAGLE 2000 glass. (a) Cross-sectional THG images (in false colors) of waveguide written with pulse energy of 110 nJ, scan speed of 0.3 mm/s alongside its transmission microscope image of the end-facet. (b) Transmission microscope end-facet image of the waveguide array written with alternate scan directions at energy of 110 nJ, scan speed of 0.3 mm/s. (c) Close-up THG image of the bottom region of the waveguide array.

For integrated components working at 800 nm wavelength in Corning EAGLE 2000 glass, we normally use 85 nJ pulse energy and 2 mm/s scan speed to fabricate them, after taking waveguide propagation loss, near field mode profile, polarization property, fabrication efficiency and so on into account. The quill effect under these optimized writing parameters is normally not as striking as that shown in Fig. 3, but it is still visible under the THG microscope and more importantly it has noticeable impact on the properties of some FLW-PIC components. As an example, cross-sectional THG image at the coupling region of a 3D tritter, which was written with the optimized writing parameters in Corning EAGLE 2000 glass, is shown in Fig. 4. From Fig. 4 one can see the quill effect in particular at the bottom regions (highlighted by dot-dashed rectangles) of the three coupling waveguides W1, 2 and 3. The quill effect effectively shifts the waveguide light-guiding center positions differently for the waveguides written with opposite directions. Therefore, as we have demonstrated in reference [32], when the three waveguide are written with different scan directions, like the one shown in Fig. 4, the beam-splitting ratios of the tritter will be affected by quill effect, bearing in mind that the output beam-splitting ratios of a tritter is very sensitive to the relative light-guiding center positions between three coupling waveguides at its coupling region.

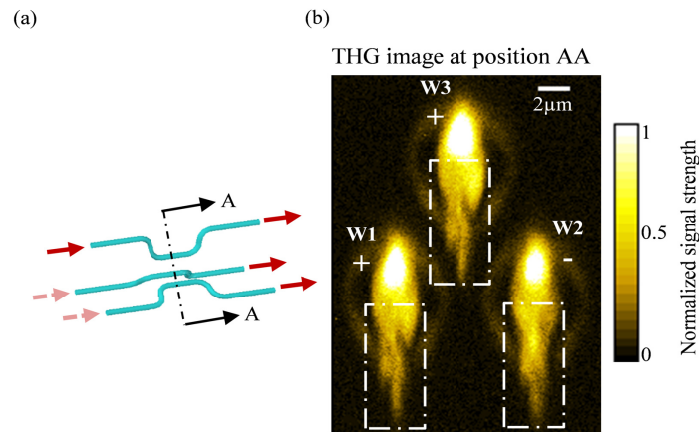


Fig. 4. A tritter written in EAGLE 2000 glass. (a) Schematic of tritter. (b) Cross-sectional THG image of a tritter (in false color) written with pulse energy of 85 nJ and scan speed of 2 mm/s; W1, 2, 3 denote waveguide 1, 2, 3, which were written with alternate scan directions represented by '+' and '-'.

3. Summary

With the help of adaptive THG microscopy, we have revealed the quill effect and studied its influence on the performance of the fabricated FLW-PIC components in low-loss-waveguide writing regime, both in fused silica and borosilicate glass. This study not only gives us new phenomenological insight into the quill effect in a previously un-explored fabrication regime, but more importantly the information provided is critical for fabricating FLW-PIC components for some highly demanding applications like polarization-dependent or multi-photon-interference-based quantum information processing. The quill effect can be reduced through control the spatial intensity distribution of writing beam demonstrated by Salter et al [6], or can be avoided by simply using the same scan direction for all scans.

Funding

UK Engineering and Physical Sciences Research Council (EPSRC) EP/M013243/1 and EP/K034480/1.

References

1. P. Kazansky, W. Yang, E. Bricchi, J. Bovatsek, A. Arai, Y. Shimotsuma, K. Miura, and K. Hirao, "Quill" writing with ultrashort light pulses in transparent materials," *Appl. Phys. Lett.* **90**(15), 151120 (2007).
2. B. Pommellec, L. Sudrie, M. Franco, B. Prade, and A. Mysyrowicz, "Femtosecond laser irradiation stress induced in pure silica," *Opt. Express* **11**(9), 1070–1079 (2003).
3. W. Yang, P. G. Kazansky, Y. Shimotsuma, M. Sakakura, K. Miura, and K. Hirao, "Ultrashort-pulse laser calligraphy," *Appl. Phys. Lett.* **93**(17), 171109 (2008).
4. D. N. Vitek, E. Block, Y. Bellouard, D. E. Adams, S. Backus, D. Kleinfeld, C. G. Durfee, and J. A. Squier, "Spatio-temporally focused femtosecond laser pulses for nonreciprocal writing in optically transparent materials," *Opt. Express* **18**(24), 24673–24678 (2010).
5. A. Patel, Y. Svirko, C. Durfee, and P. G. Kazansky, "Direct Writing with Tilted-Front Femtosecond Pulses," *Sci. Rep.* **7**(1), 12928 (2017).
6. P. S. Salter and M. J. Booth, "Dynamic control of directional asymmetry observed in ultrafast laser direct writing," *Appl. Phys. Lett.* **101**(14), 141109 (2012).
7. Y. Bellouard and M.-O. Hongler, "Femtosecond-laser generation of self-organized bubble patterns in fused silica," *Opt. Express* **19**(7), 6807–6821 (2011).
8. C. Corbari, A. Champion, M. Gecevičius, M. Beresna, Y. Bellouard, and P. G. Kazansky, "Femtosecond versus picosecond laser machining of nano-gratings and micro-channels in silica glass," *Opt. Express* **21**(4), 3946–3958 (2013).
9. H. Song, Y. Dai, J. Song, H. Ma, X. Yan, and G. Ma, "Femtosecond laser-induced structural difference in fused silica with a non-reciprocal writing process," *Appl. Phys., A Mater. Sci. Process.* **123**(4), 255 (2017).

10. D. Tan, K. N. Sharafudeen, Y. Yue, and J. Qiu, "Femtosecond laser induced phenomena in transparent solid materials: Fundamentals and applications," *Prog. Mater. Sci.* **76**, 154–228 (2016).
11. A. Crespi, R. Ramponi, R. Osellame, L. Sansoni, I. Bongioanni, F. Sciarrino, G. Vallone, and P. Mataloni, "Integrated photonic quantum gates for polarization qubits," *Nat. Commun.* **2**(1), 566 (2011).
12. L. Sansoni, F. Sciarrino, G. Vallone, P. Mataloni, A. Crespi, R. Ramponi, and R. Osellame, "Two-Particle Bosonic-Fermionic Quantum Walk via Integrated Photonics," *Phys. Rev. Lett.* **108**(1), 010502 (2012).
13. G. Corrielli, A. Crespi, R. Geremia, R. Ramponi, L. Sansoni, A. Santinelli, P. Mataloni, F. Sciarrino, and R. Osellame, "Rotated waveplates in integrated waveguide optics," *Nat. Commun.* **5**(1), 4249 (2014).
14. I. Pitsios, L. Banchi, A. S. Rab, M. Bentivegna, D. Caprara, A. Crespi, N. Spagnolo, S. Bose, P. Mataloni, R. Osellame, and F. Sciarrino, "Photonic simulation of entanglement growth and engineering after a spin chain quench," *Nat. Commun.* **8**(1), 1569 (2017).
15. J. Zeuner, A. N. Sharma, M. Tillmann, R. Heilmann, M. Gräfe, A. Moqanaki, A. Szameit, and P. Walther, "Integrated-optics heralded controlled-NOT gate for polarization-encoded qubits," *npj Quantum Inf.* **4**(13), 1–12 (2018).
16. A. Jesacher, A. Thayil, K. Grieve, D. Débarre, T. Watanabe, T. Wilson, S. Srinivas, and M. Booth, "Adaptive harmonic generation microscopy of mammalian embryos," *Opt. Lett.* **34**(20), 3154–3156 (2009).
17. G. D. Marshall, A. Jesacher, A. Thayil, M. J. Withford, and M. Booth, "Three-dimensional imaging of direct-written photonic structures," *Opt. Lett.* **36**(5), 695–697 (2011).
18. M. Müller, J. Squier, K. R. Wilson, and G. J. Brakenhoff, "3D microscopy of transparent objects using third-harmonic generation," *J. Microsc.* **191**(3), 266–274 (1998).
19. J. Guan, X. Liu, P. S. Salter, and M. J. Booth, "Hybrid laser written waveguides in fused silica for low loss and polarization independence," *Opt. Express* **25**(5), 4845–4859 (2017).
20. L. B. Jeunhomme, *Single-Mode Fiber Optics Principles and Applications* (Marcel Dekker, Inc 1990).
21. V. R. Bhardwaj, P. B. Corkum, D. M. Rayner, C. Hnatovsky, E. Simova, and R. S. Taylor, "Stress in femtosecond-laser-written waveguides in fused silica," *Opt. Lett.* **29**(12), 1312–1314 (2004).
22. Y. Shimotsuma, P. G. Kazansky, J. Qiu, and K. Hirao, "Self-organized nanogratings in glass irradiated by ultrashort light pulses," *Phys. Rev. Lett.* **91**(24), 247405 (2003).
23. R. S. Taylor, E. Simova, and C. Hnatovsky, "Creation of chiral structures inside fused silica glass," *Opt. Lett.* **33**(12), 1312–1314 (2008).
24. W. Yang, E. Bricchi, P. G. Kazansky, J. Bovatsek, and A. Y. Arai, "Self-assembled periodic sub-wavelength structures by femtosecond laser direct writing," *Opt. Express* **14**(21), 10117–10124 (2006).
25. J. Sakai and T. Kimura, "Birefringence and polarization characteristics of single-mode optical fibers under elastic deformations," *IEEE J. Quantum Electron.* **17**(6), 1041–1051 (1981).
26. J. Sakai and T. Kimura, "Birefringence caused by thermal stress in elliptically deformed core optical fibers," *IEEE J. Quantum Electron.* **18**(11), 1899–1909 (1982).
27. A. Crespi, R. Osellame, R. Ramponi, V. Giovannetti, R. Fazio, L. Sansoni, F. De Nicola, F. Sciarrino, and P. Mataloni, "Anderson localization of entangled photons in an integrated quantum walk," *Nat. Photonics* **7**(4), 322–328 (2013).
28. A. Crespi, R. Osellame, R. Ramponi, D. J. Brod, E. F. Galvão, N. Spagnolo, C. Vitelli, E. Maiorino, P. Mataloni, and F. Sciarrino, "Integrated multimode interferometers with arbitrary designs for photonic boson sampling," *Nat. Photonics* **7**(7), 545–549 (2013).
29. T. Giordani, F. Flamini, M. Pompili, N. Viggianiello, N. Spagnolo, A. Crespi, R. Osellame, N. Wiebe, M. Walschaers, A. Buchleitner, and F. Sciarrino, "Experimental statistical signature of many-body quantum interference," *Nat. Photonics* **12**(3), 173–178 (2018).
30. W.-J. Chen, S. M. Eaton, H. Zhang, and P. R. Herman, "Broadband directional couplers fabricated in bulk glass with high repetition rate femtosecond laser pulses," *Opt. Express* **16**(15), 11470–11480 (2008).
31. S. M. Eaton, H. Zhang, M. L. Ng, J. Li, W.-J. Chen, S. Ho, and P. R. Herman, "Transition from thermal diffusion to heat accumulation in high repetition rate femtosecond laser writing of buried optical waveguides," *Opt. Express* **16**(13), 9443–9458 (2008).
32. J. Guan, X. Liu, A. J. Menssen, and M. J. Booth, "Microscopic characterization of laser-written phenomena for component-wise testing of photonic integrated circuits," <https://arxiv.org/abs/1802.08016>.